# A Role for Lipid Rafts in B Cell Antigen Receptor Signaling and Antigen Targeting

By Paul C. Cheng,* Michelle L. Dykstra,* Richard N. Mitchell,‡ and Susan K. Pierce*

*From the *Department of Biochemistry, Molecular Biology, and Cell Biology, Northwestern University, Evanston, Illinois 60208; and the ‡Immunology Research Division, Department of Pathology, Brigham and Women's Hospital and Harvard Medical School, Boston, Massachusetts 02115*

## Summary

The B cell antigen receptor (BCR) serves both to initiate signal transduction cascades and to target antigen for processing and presentation by MHC class II molecules. How these two BCR functions are coordinated is not known. Recently, sphingolipid- and cholesterol-rich plasma membrane lipid microdomains, termed lipid rafts, have been identified and proposed to function as platforms for both receptor signaling and membrane trafficking. Here we show that upon cross-linking, the BCR rapidly translocates into ganglioside $G_{M1}$-enriched lipid rafts that contain the Src family kinase Lyn and exclude the phosphatase CD45R. Both Igα and Lyn in the lipid rafts become phosphorylated, and subsequently the BCR and a portion of $G_{M1}$ are targeted to the class II peptide loading compartment. Entry into lipid rafts, however, is not sufficient for targeting to the antigen processing compartments, as a mutant surface Ig containing a deletion of the cytoplasmic domain is constitutively present in rafts but when cross-linked does not internalize to the antigen processing compartment. Taken together, these results provide evidence for a role for lipid rafts in the initial steps of BCR signaling and antigen targeting.

Key words: membrane microdomain • B lymphocyte • immunoglobulin • Igα/Igβ • endocytosis

The B cell antigen receptor (BCR)[1] is a multicomponent complex on the cell surface that is composed of a cell surface (s)Ig that mediates antigen binding and a noncovalently associated heterodimer, Igα/Igβ, that functions as a signal transduction complex (for review see reference 1). After antigen binding and cross-linking, the BCR transmits signals through several signaling pathways that result in the expression of a variety of genes associated with B cell activation. Early key events in the BCR signal transduction cascade include the activation of protein tyrosine kinases of the Src and Syk/Zap70 families and the phosphorylation of tyrosine residues in the immune receptor tyrosine-based activation motifs (ITAMs) in the cytoplasmic domains of Igα and Igβ (1–3).

Although necessary for the activation of B cells, the signals transmitted through the BCR alone are not sufficient to induce the proliferation and differentiation of B cells. The B cell antibody response to the vast majority of protein antigens requires B cell interaction with antigen-specific T cells (for review see reference 4). The interactions of B cells and helper T cells are dependent on the processing and presentation of antigen by B cells to the helper T cells (5). The BCR plays an important role in antigen processing by targeting bound antigen to the class II peptide loading compartment (IIPLC; for review see reference 6). Indeed, BCR-mediated antigen processing is thousandsfold more efficient in B cells compared with the processing of antigen taken up nonspecifically by fluid phase pinocytosis.

Recent evidence indicates that the two functions of the BCR, signaling and antigen targeting, are interrelated (7). Monovalent antigens bound to the BCR are processed and presented, but less efficiently than multivalent antigens (8). Cross-linking the BCR results in internalization of a larger number of receptors and a significant acceleration of the targeting of the BCR to the IIPLC and of the degradation of BCR and bound antigen (9). The accelerated delivery of antigen to the IIPLC may play an important role in vivo during periods of rapid antigen-driven B cell expansion and T cell–dependent selection. The effects of BCR cross-linking appear to be the result of BCR signaling rather than ag-

M.L. Dykstra and P.C. Cheng contributed equally to this work.

[1]*Abbreviations used in this paper:* BCR, B cell antigen receptor; CM, complete media; CTB, cholera toxin B subunit; ECL, enhanced chemiluminescence; GPI, glycosylphosphatidylinositol; HRP, horseradish peroxidase; ITAMs, immune receptor tyrosine-based activation motifs; PI-PLC, phosphatidylinositol-specific phospholipase C; sIg, cell surface Ig; TfR, transferrin receptor; WT, wild-type.

 J. Exp. Med. © The Rockefeller University Press • 0022-1007/99/12/1549/12 $5.00
Volume 190, Number 11, December 6, 1999 1549–1560
http://www.jem.org

gregation of the BCR because kinase inhibitors that block BCR signaling block accelerated targeting and degradation (10). In addition, Aluvihare et al. (11) recently showed that accelerated antigen targeting by the BCR is dependent on Igα and Igβ. Further evidence for an important role of Igα/Igβ in BCR antigen targeting was demonstrated by the behavior of two mutant Igs that do not associate with Igα/Igβ (12). An sIg in which the short, three–amino acid cytoplasmic domain was deleted (μCytoΔ) was expressed on the cell surface without Igα/Igβ. The μCytoΔ was glycosylphosphatidylinositol (GPI) linked (13) and, after antigen binding, failed to internalize and target antigen to the IIPLC (12). Another sIg in which $Y_{587}$ and $S_{588}$ in the transmembrane region was changed to VV (μYS/VV) was also expressed on the cell surface in the absence of Igα/Igβ (14). μYS/VV was competent to internalize bound antigen and, although the antigen was degraded, it was not presented by the class II molecules, suggesting that correct targeting of the BCR to the IIPLC was dependent on Igα/Igβ (15). Another sIg containing a single $Y_{587}\rightarrow F$ transmembrane mutation that associated with Igα/Igβ was signaling competent but like μYS/VV did not target antigen for processing. Thus, both the signaling function and the nature of the sIg transmembrane region appear to dictate the behavior of the BCR, that is, to specify the correct targeting of the BCR to the IIPLC and to accelerate the rate at which the antigen is targeted to the IIPLC. At the time of this writing, the molecular mechanisms by which the targeting and signaling functions of the BCR are coordinated after antigen binding and receptor cross-linking on the cell surface are not known.

Recent advances in membrane biology have led to the identification of glycosphingolipid- and cholesterol-rich plasma membrane microdomains, or lipid rafts, that have been proposed to function as platforms for both signal transduction and membrane trafficking (for review see reference 16). Lipid rafts can be isolated based on their insolubility in Triton X-100 detergent and buoyant density on sucrose gradients (17–20). Several proteins have been identified as residents of these lipid microdomains, including caveolin (21), GPI-linked membrane proteins (17, 22), influenza hemagglutinin (23), the high-affinity IgE receptor (24, 25), and the B cell integral membrane protein CD20 (26). In addition, several molecules involved in signal transduction have been shown to be associated with lipid rafts such as the Gα subunits of heterotrimeric G proteins (27), the double-acylated Src family protein tyrosine kinases Lck, Lyn, and Fyn (28), and the Zap70 family protein tyrosine kinase, Syk (25). The lipid rafts are also associated with actin and actin-binding proteins (29, 30).

Immunofluorescence microscopy (22, 31), fluorescence resonance energy transfer (32), and chemical cross-linking studies (21, 33) have led to the proposal that rafts are not static entities in situ but instead dynamic microdomains on the cell surface to which proteins and lipids have variable affinities (34). In this way, certain signals such as the cross-linking of a membrane protein may affect its distribution in raft domains (35). Indeed, it has been shown recently that upon cross-linking the TCR, its associated signaling molecules and coreceptors acquire increased affinities toward lipid rafts (36–40) and that the integrity of these domains is required for efficient signal transduction by the TCR (37). Here we provide evidence for a role for lipid rafts in BCR signaling and antigen targeting.

## Materials and Methods

*Cell Lines and Antibodies.* The mouse B cell lymphoma CH27 ($H\text{-}2^k$, $IgM^+$, $Fc\gamma RIIB1^-$) was maintained in DME supplemented as previously described (41) and containing 15% FCS (15% complete media [CM]). The A20 B lymphoma line ($H\text{-}2^d$, $IgG_{2a}{}^+$, $Fc\gamma RIIB1^+$) stably transfected with either a human μ wild-type (A20μWT) or a mutation that generated a premature stop codon at amino acid $K_{595}$, resulting in the deletion of the cytoplasmic tail (A20μCytoΔ; reference 12), was maintained in 15% CM containing 600 μg/ml G418.

Goat Fab anti–mouse μ chain; rabbit anti–human IgG plus IgM (H and L chain); horseradish peroxidase (HRP)-conjugated goat anti–mouse IgG plus IgM (H and L chain); HRP-conjugated rabbit $F(ab')_2$ anti–mouse γ chain and anti–human μ chain; and FITC-conjugated goat anti–mouse γ chain, anti–human γ chain, and anti–human μ chain were purchased from Jackson ImmunoResearch. Cholera toxin B subunit (CTB) conjugated to HRP and methyl-β-cyclodextrin were obtained from Sigma Chemical Co. Antibodies specific for mouse CD45R and Lyn were obtained from PharMingen. The goat polyclonal antibody specific for actin was obtained from Santa Cruz Biotechnology, and the rat mAb YL1/2 specific for tubulin (42) was a gift from Dr. Douglas T. Fearon (University of Cambridge, UK). RC20H phosphotyrosine-specific recombinant antibody conjugated to HRP was purchased from Transduction Labs. Polyclonal antibodies specific for H2-M were generated in rabbits using a peptide representing the cytoplasmic tail domain of H2-M (residues 224–245) containing a T cell epitope derived from tetanus toxoid (residues 582–599). The mouse $IgG_{2a}$ hybridoma 17.3.3s producing an mAb specific for $I\text{-}E^k$, the mouse $IgG_{2a}$ hybridoma HB3 (MK-D6) producing an mAb specific for $I\text{-}A^d$, and the rat $IgG_{2a}$ hybridoma RI7 217.1.3 producing an mAb specific for the transferrin receptor (TfR) were obtained from the American Tissue Type Culture Collection. The rat hybridoma 79a3, producing an $IgG_1$ mAb specific for the cytosolic domain of mouse Igα, was generated and characterized in the Pierce laboratory at Northwestern University. All hybridomas were maintained in the Pierce laboratory, and mAbs were purified from culture supernatant by affinity chromatography.

Goat Fab anti–mouse μ was iodinated using the iodine monochloride method to a specific activity of $0.5\text{–}1.0 \times 10^7$ cpm/μg as described (43). More than 85% of the $^{125}$I–Fab was precipitated by 10% TCA, indicating little free $^{125}$I. Unlabeled Fab competed with $^{125}$I–Fab for binding to the surface of CH27 cells, indicating that iodination did not affect the binding properties of the Fab.

*Isolation of Lipid Rafts.* Lipid rafts were isolated using modified lysis conditions and flotation on discontinuous sucrose gradients (20, 36, 37). In brief, cells ($10^8$) were washed with ice-cold PBS and lysed for 30 min on ice in 1% Triton X-100 in TNEV containing protease and phosphatase inhibitors (TNEV: 10 mM Tris/HCl, pH 7.5, 150 mM NaCl, and 5 mM EDTA; CLAP [2.5 mg/ml each of chymostatin, leupeptin, antipain, and pepstatin A in DMSO] and 1 mM sodium orthovanadate). The lysis solution was further homogenized with ten strokes in a Wheaton loose-fitting dounce homogenizer. Nuclei and cellular debris were pel-

leted by centrifugation at 900 *g* for 10 min. For the discontinuous sucrose gradient, 1 ml of cleared supernatant was mixed with 1 ml of 85% sucrose in TNEV and transferred to the bottom of a Beckman 14 × 89 mm centrifuge tube. The diluted lysate was overlaid with 6 ml 35% sucrose in TNEV and finally 3.5 ml 5% sucrose in TNEV. The samples were centrifuged in an SW41 rotor at 200,000 *g* for 16–20 h at 4°C. 1-ml fractions were collected from the top of the gradient.

*Measurement of HRP Activity.* A 50-μl sample of each fraction from the discontinuous sucrose gradient was incubated with 50 μl of substrate solution (5 mg/ml 2,2-azino-bis-3-ethylbenzthiazoline-6-sulfonic acid in 0.1 M citrate-phosphate buffer, pH 4.0, with 0.015% $H_2O_2$). The absorbence was measured at 405 nm on an ELISA plate reader.

*Surface Biotinylation and Metabolic Labeling.* Cells ($2 \times 10^8$) were washed with ice-cold $HBSS^+$ (13 mM $CaCl_2$, 50 mM KCl, 5 mM $MgCl_2.6H_2O$, 4 mM $MgSO_4$, 1.38 M NaCl, 56 mM glucose, and 200 mM Hepes, pH 7.4) and incubated in 0.2 mg/ml *N*-hydroxysuccinimide long chain–biotin (Pierce Chemical Co.) in $HBSS^+$ for 15 min at 4°C. Additionally, an equal volume of 0.2 mg/ml biotin was added, and incubation at 4°C was continued for another 15 min. The biotinylation reaction was quenched with ice-cold DME/BSA, washed extensively, and resuspended in 5 ml DME/BSA. For metabolic labeling, cells ($2 \times 10^8$) were starved for 30 min in $Met^-/Cys^-$ DME with 5% dialyzed FCS (5% labeling media) and labeled for 15 min with 200 μCi/ml $^{35}S$–70% methionine/30% cysteine (NEN Express).

*HRP–3,3′-Diaminobenzidine Reaction.* Cells were washed twice with ice-cold $HBSS^+$ and resuspended in 1 ml of 0.5 mg/ml 3,3′-diaminobenzidine (DAB) in $HBSS^+$ with or without 0.1% $H_2O_2$. The cells were incubated for 45 min at 4°C, washed with ice-cold $HBSS^+$, and lysed in 1 ml of lysis buffer for 30 min on ice. For studies on class II colocalization, 1% Triton X-100 lysis buffer was used (1% Triton X-100, 50 mM Tris/HCl, pH 7.4, 150 mM NaCl, 5 mM EDTA, 0.02% sodium azide, and CLAP). For studies on colocalization with biotinylated surface proteins, RIPA lysis buffer was used (1% Triton X-100, 0.5% deoxycholate, and 0.1% SDS in PBS with 0.02% sodium azide and CLAP). Cellular debris and aggregated protein polymers were pelleted from the lysate with a 30-min 14,000 *g* microfuge spin before immunoprecipitation.

*Treatment of Cells with Phosphatidylinositol-specific Phospholipase C.* Cells ($10^7$) were surface biotinylated as described above and washed twice in ice-cold PBS. Phosphatidylinositol-specific phospholipase C (PI-PLC; Sigma Chemical Co.) was added at a concentration of 1 U/ml PBS and incubated at 37°C for 1 h. Cells were pelleted and the supernatant collected. The cells were then washed twice with ice-cold PBS before lysis in 1 ml 1% Triton X-100 lysis buffer. The lysates were cleared of debris as described above. The cell lysates and the supernatants were immunoprecipitated for human Ig, and biotinylated material was visualized by immunoblotting as described below.

*Immunoprecipitation and Immunoblotting.* Cell lysates were precleared of nonspecific proteins and endogenous Ig by incubation with a 30% slurry of protein A–Sepharose or protein G–Sepharose (Amersham Pharmacia Biotech) at 4°C for 1 h. Antibodies (10 μg) and beads (50 μl) were added to the cleared lysate and incubated overnight. The beads were washed three times with lysis buffer and once with PBS. Samples were eluted from the beads by either reducing and boiling for 5 min or incubating with a cocktail lacking reducing agent at room temperature for 30 min. The samples were subjected to 10% SDS-PAGE. Gels with metabolically labeled samples were dried and exposed to film, and gels with biotinylated samples were transferred onto Millipore Immobilon PVDF (polyvinylidene difluoride) membrane. The membranes were blocked for 1 h at 25°C in a buffer containing 0.5% Tween-20, 18% glucose, and 10% glycerol in PBS (TGG) with 3% milk and 1% BSA. The blots were washed in PBS/0.1% Tween-20. A 1:1000 dilution of streptavidin–HRP (Amersham Pharmacia Biotech) in TGG containing 0.3% BSA was added and incubated at 25°C for 1 h. After washing with PBS/Tween-20, the blots were visualized with enhanced chemiluminescence (ECL; Amersham Pharmacia Biotech). All films were quantified by densitometry.

## Results

*Cross-linking the BCR Results in its Rapid Translocation into Lipid Rafts.* The present evidence indicates that the plasma membrane contains sphingolipid- and cholesterol-enriched microdomains, or lipid rafts, proposed to play a role in membrane trafficking and signal transduction. These microdomains are resistant to Triton X-100 detergent solubilization, allowing for their isolation in discontinuous sucrose density gradients. The location of the BCR in unactivated B cells and after BCR cross-linking with regard to lipid rafts was determined. The CH27 B lymphoma cells that were surface biotinylated were either untreated or treated with anti-Ig at 4°C for 15 min, washed, and warmed to 37°C for 0 or 30 min. The cells were lysed in 1% Triton X-100 lysis buffer on ice, and the lysates were subjected to discontinuous sucrose density gradient centrifugation. Individual fractions from the gradient were subjected to SDS-PAGE and immunoblotting. The position of the lipid rafts in the sucrose gradient was determined by the presence of the ganglioside $G_{M1}$, detected using $G_{M1}$-specific ligand CTB (Fig. 1). As shown in Fig. 1, $G_{M1}$ is enriched in the fractions at the top of the sucrose gradient, fractions 3–6. There was no detectable $G_{M1}$ in fractions 7–9 and only a small amount of $G_{M1}$ in the solubilized material located at the bottom of the gradient, fractions 10–12, indicating a clear separation of the lipid rafts from the Triton X-100–soluble membranes and components. To determine where in the gradients the BCR resided, immunoblots were probed with antibodies specific for mouse IgM and an mAb specific for Igα. In untreated cells, Ig and Igα were found in the soluble fractions of the sucrose gradient and not in the detergent-insoluble lipid raft region, indicating that in resting cells the BCR is excluded from the lipid rafts (Fig. 1). After BCR cross-linking, a significant portion of both the Ig and Igα are translocated into the lipid raft regions of the sucrose gradient. Both Ig and Igα are present in the lipid rafts immediately after cross-linking and warming to 37°C. Somewhat less Ig and Igα are detected in the lipid raft region 30 min after cross-linking.

To determine where in the gradient fractions the surface BCR resided, the position of biotinylated sIg and sIgα was examined. The biotinylated CH27 lymphoma cells were either untreated or treated with anti-Ig and analyzed as described above. Biotinylated proteins were immunoprecipitated from the Triton X-100 detergent lysates using strepta-

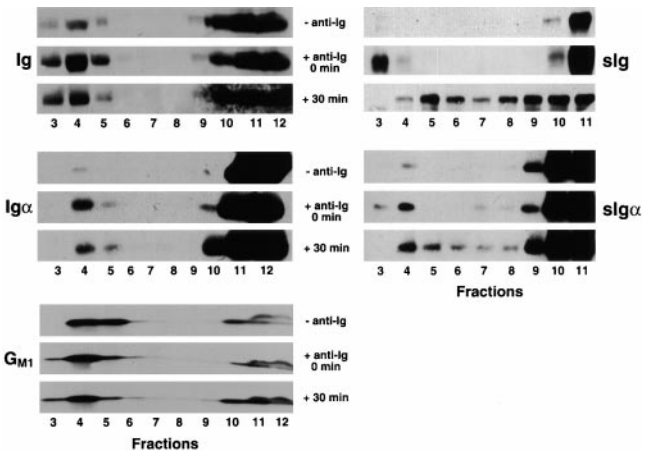


**Figure 1.** BCR cross-linking results in translocation of the BCR into $G_{M1}$-containing lipid rafts. CH27 cells were surface biotinylated at 4°C and incubated with anti-Ig on ice for 15 min. The cells were warmed for 0 or 30 min and lysed in 1% Triton X-100 in TNEV buffer. The lysates were subjected to discontinuous sucrose density gradient centrifugation, and 1-ml fractions were collected. To determine the location of lipid rafts in the gradient, 100 μl of the individual fractions were subjected to 10% SDS-PAGE. After transfer onto PVDF, the membranes were probed for the presence of μ heavy chain and Igα using specific antibodies. The ganglioside $G_{M1}$ was detected using CTB–HRP. To determine the location of surface BCR in the gradient, biotinylated proteins were immunoprecipitated from the gradient fractions using streptavidin–agarose. The immunoprecipitates were subjected to 10% SDS-PAGE and immunoblot probing with antibodies specific for Ig and Igα detected with HRP-conjugated secondary antibodies and ECL. Representative blots of three separate experiments are shown.

vidin–agarose, and the immunoprecipitates were analyzed by SDS-PAGE and immunoblot probing with antibodies specific for Ig or Igα. The distribution of the surface BCR is similar to that observed for total cellular BCR. In the absence of anti-Ig cross-linking, the biotinylated sIg is excluded from the lipid raft and is found in the detergent-soluble region of the gradient. Immediately upon cross-linking, the biotinylated sIg is found in the raft region, where it persists for at least 30 min. The behavior of biotinylated sIgα is similar to that of sIg, being excluded from lipid rafts in the absence of cross-linking by anti-Ig and included in lipid rafts upon cross-linking. Thus, cross-linking the BCR with anti-Ig results in the rapid translocation of the surface BCR into plasma membrane lipid rafts.

*Lipid Rafts Include the Kinase Lyn and Exclude the Phosphatase CD45R.* The results of experiments described above indicate that upon cross-linking, the BCR is rapidly translocated into lipid rafts. As stated above, BCR cross-linking results in the initiation of a signal transduction cascade involving the phosphorylation of Igα/Igβ ITAM tyrosines. The Src family kinase Lyn is an essential protein tyrosine kinase involved in the initial phosphorylation events. The BCR response is ultimately terminated by dephosphorylation of BCR signaling components involving plasma membrane phosphatases such as CD45R. Thus, the location of Lyn and CD45R in membrane fractions was determined in unactivated and activated B cells. B cells were untreated or incubated with anti-Ig at 4°C for 30 min, washed, and warmed to 37°C for 0 or 30 min. The cells were lysed in 1% Triton X-100 lysis buffer and subjected to discontinuous sucrose gradient centrifugation, and the gradient fractions were analyzed by SDS-PAGE and immunoblotting for the presence of Lyn and CD45R. The kinase Lyn is concentrated in the lipid raft region of the gradient in resting cells and remains in rafts after BCR cross-linking, at least for the 30-min time course of this experiment (Fig. 2). In contrast, the phosphatase CD45R is excluded from the lipid rafts in resting cells and remains excluded after BCR cross-linking (Fig. 2). The location of H2-M, a class II–like protein that at steady state has been shown to reside primarily in the IIPLC in CH27 cells (44), was also determined. As anticipated, H2-M was found in the Triton X-100–soluble membrane fractions in resting cells, and its presence in soluble membranes did not change upon BCR cross-linking. A portion of the cytoskeleton protein actin was found to be constitutively associated with lipid rafts (Fig. 2). In contrast, tubulin was found to be completely excluded from the lipid rafts in both anti-Ig–treated and untreated cells.

*Phosphorylated Igα and Lyn Are Present in Lipid Rafts after BCR Cross-linking.* The presence of Lyn in the lipid raft suggests that the Igα present in the lipid rafts after BCR cross-linking may be phosphorylated. To determine the plasma membrane location of phosphorylated proteins, B cells were untreated or treated with anti-Ig at 4°C and warmed to 37°C for 0, 10, or 30 min. At the end of each time point, the cells were lysed in 1% Triton X-100 lysis buffer and subjected to discontinuous sucrose density gradient centrifugation. The gradient fractions were analyzed by SDS-PAGE and immunoblot probing for phosphotyrosine-containing proteins using the phosphotyrosine-specific recombinant antibody RC20H. In the absence of cross-linking, phosphorylated proteins are present in the Triton X-100–soluble membrane fractions, and only faint bands of phos-

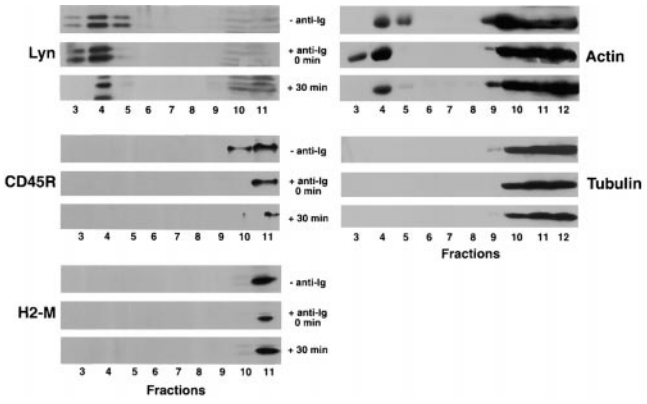


**Figure 2.** The kinase Lyn is constitutively present and the phosphatase CD45R is excluded from rafts in B cells. CH27 cells were treated with anti-Ig at 4°C for 15 min, washed, and warmed for 0 or 30 min at 37°C. The cells were lysed in 1% Triton X-100 in TNEV, and lysates were subjected to discontinuous sucrose gradient centrifugation. Fractions from the gradient were subjected to 10% SDS-PAGE and transferred to PVDF. To determine the positions in the gradient of Lyn, CD45R, H2-M, actin, and tubulin, the membranes were probed with specific antibodies followed by HRP-conjugated secondary antibodies and ECL. Shown are representative blots of three separate experiments.

phorylated proteins can be detected in the lipid raft region of the gradient (Fig. 3), reflecting the constitutive level of protein tyrosine phosphorylation in CH27 cells. Upon BCR cross-linking, the intensity and number of phosphorylated proteins increase immediately in the fractions that contain detergent-soluble and -insoluble membranes and then return to the levels present in unactivated cells by 30 min. To determine if the phosphorylated proteins in the lipid rafts include either Igα or Lyn, immunoblots were reprobed with antibodies specific for Igα and Lyn. As shown, the Igα band at 34 kD and the Lyn bands at 53 and 56 kD align with phosphotyrosine-containing proteins (Fig. 3). By immunoblotting, Lyn appears to be present in the lipid rafts in approximately the same amount in untreated and anti-Ig–treated cells throughout the 30-min chase; however, the phosphorylation state of Lyn appears to change with BCR cross-linking. Igα enters the raft after BCR cross-linking, with maximal translocation occurring 10 min after BCR cross-linking; by 30 min, the amount of Igα in lipid rafts decreases. At each time point, the Igα present in the raft region appears to be phosphorylated. It is difficult to determine if Lyn and Igα phosphorylation is restricted to the lipid rafts because of the complexity of the pattern of phosphorylated proteins in the Triton X-100–soluble fractions, although there are no obvious phosphoproteins aligning with Igα and Lyn. Taken together, these results suggest that after cross-linking, the BCR enters the lipid rafts, where the Lyn kinase is concentrated to facilitate initiation of signal cascades, including Igα and Lyn phosphorylation. The exclusion of CD45R from the lipid rafts indicates that only BCRs outside the lipid rafts would be targets of CD45R phosphatase activity.

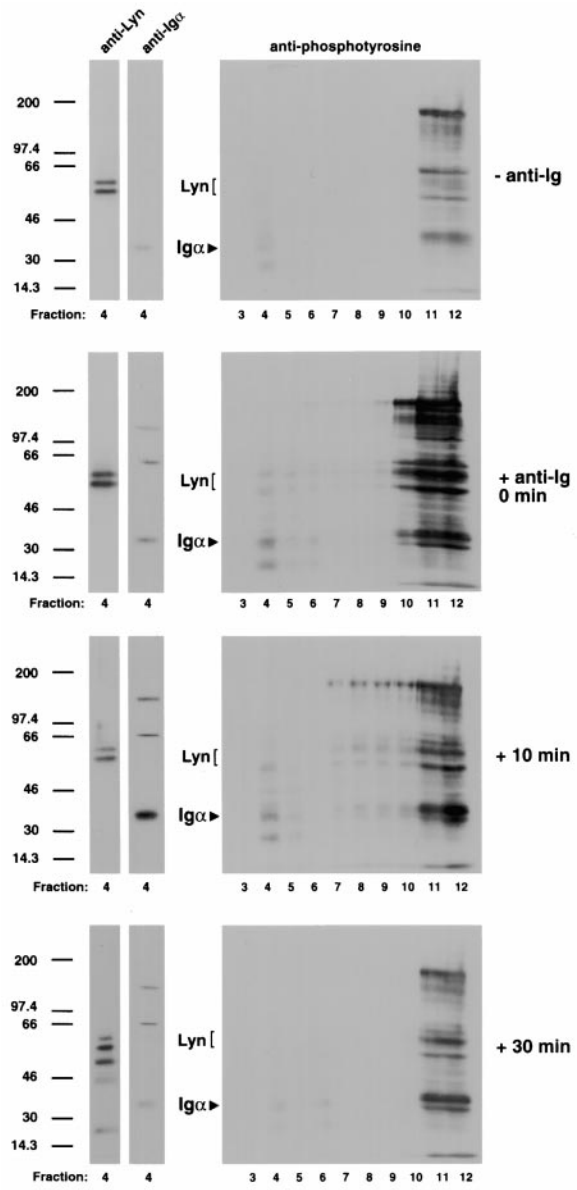


**Figure 3.** Phosphorylated Igα and Lyn are present in lipid rafts after BCR cross-linking. CH27 cells were untreated or incubated with anti-Ig for 30 min at 4°C and warmed to 37°C for 0, 10, or 30 min. Cells were lysed in 1% Triton X-100 in TNEV buffer and subjected to discontinuous sucrose density gradient centrifugation. Right panels: gradient fractions were subjected to SDS-PAGE and immunoblot probing with the HRP-conjugated, phosphotyrosine-specific recombinant Ab RC20H and visualized by ECL. Left panels: immunoblots were treated with 0.02% sodium azide to inhibit RC20H enzyme activity, reprobed with Igα- and Lyn-specific mAbs, and detected using HRP-conjugated secondary antibodies and ECL. Shown are the immunoblots from fraction 4. Representative blots of three separate experiments are shown.

*Antigen Bound to the BCR Is Rapidly Translocated to Lipid Rafts after BCR Cross-linking.* The results described above provide evidence that upon cross-linking, the BCR rapidly translocates into lipid rafts. To verify that the BCR that moved into lipid rafts was the BCR bound to anti-Ig as a surrogate antigen, B cells were untreated or treated with HRP–anti-Ig at 4°C for 15 min, washed, and warmed at 37°C for 0, 15, or 30 min. The cells were lysed in 1% Triton X-100 lysis buffer and subjected to discontinuous sucrose gradient centrifugation, and the HRP activity in the gradient fractions was measured (Fig. 4 A). In untreated cells, there was little endogenous peroxidase activity detected in the lipid raft region of the gradient, and a small amount of endogenous peroxidase activity was detected in the soluble membrane fractions at the bottom of the gradient. In HRP–anti-Ig–treated cells, HRP activity was found to be highly concentrated in the lipid raft regions immediately after warming to 37°C. There appears to be a slight increase in the HRP activity in the lipid raft regions 15 min after warming to 37°C and a small decrease in HRP activity after 30 min. However, the enzyme activity was not measured in a quantitative fashion, so the small differences may not be significant.

To gain a more quantitative measure of the translocation of the antigen bound to the BCR into lipid rafts, B cells were incubated for 1 h with monovalent $^{125}$I–Fab–anti-Ig and subsequently left untreated or treated with rabbit anti–mouse Ig and warmed to 37°C for 0–30 min (Fig. 4 B). In the absence of cross-linking, ~12% of the $^{125}$I–Fab–anti-Ig is located in lipid rafts. After cross-linking, this percentage increases to ~26% and then decreases to 18% by 30 min after cross-linking. The presence of the 12% of $^{125}$I–Fab in

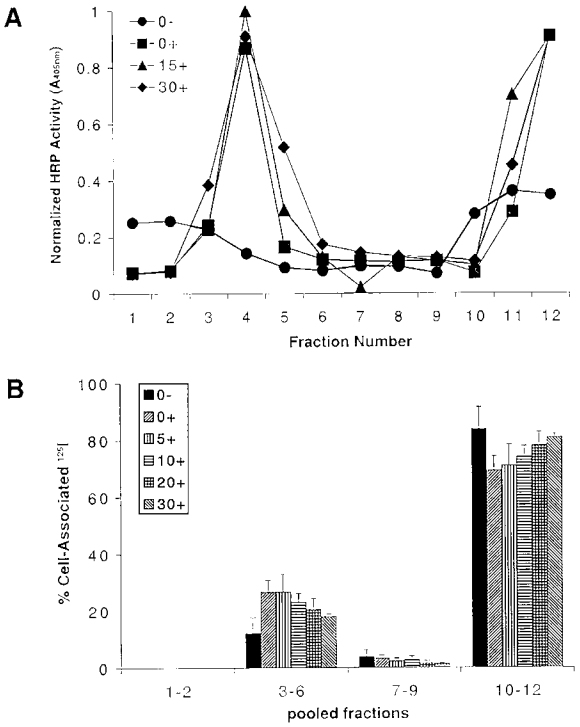


**Figure 4.** BCR-bound antigens translocate into rafts after BCR cross-linking. (A) B cells were untreated (0−) or treated with HRP–anti-Ig at 4°C for 1 h, washed, and warmed to 37°C for 0, 15, or 30 min (0+, 15+, and 30+, respectively). The cells were lysed in 1% Triton X-100 in TNEV buffer, the lysates subjected to discontinuous sucrose density gradient centrifugation, and the fractions assayed for HRP activity. (B) CH27 cells were incubated at 4°C for 1 h with $^{125}$I–Fab–anti-Ig. During the last 30 min of incubation, the cells were untreated (0−) or treated with anti-Ig to cross-link the BCR and then warmed to 37°C for 0–30 min (0+ to 30+). The cells were lysed in 1% Triton X-100 in TNEV buffer, the lysates were subjected to discontinuous sucrose gradient centrifugation, and the cpm of each fraction was measured and expressed as a percent of the total cell-associated $^{125}$I. The average and SEM of three independent experiments is shown.

the lipid rafts in unactivated cells, even though sIg and Igα were not detected in lipid rafts by immunoblotting (Fig. 1), suggests that the $^{125}$I–Fab–anti-Ig preparation likely contained some aggregated Fab–anti-Ig or F(ab′)$_2$–anti-Ig capable of cross-linking the BCR. Nevertheless, the increase in the percentage of $^{125}$I–Fab–anti-Ig in rafts after anti-Ig treatment correlated with the translocation of biotinylated sIg and Igα and HRP–anti-Ig into lipid rafts.

*BCR Cross-linking Triggers the Targeting of $G_{M1}$ to the IIPLC.* Using a nondisruptive chemical cross-linking technique, we previously showed that upon cross-linking the BCR is rapidly targeted from the plasma membrane through TfR-containing early endosomes to the IIPLC (45). To determine if the BCR remains associated with components of the lipid raft during intracellular targeting, the same chemical cross-linking technique was used to follow the intracellular movement of the lipid raft ganglioside $G_{M1}$ in untreated B cells and in B cells treated with anti-Ig. CTB–HRP was used to label $G_{M1}$ at the B cell surface at 4°C and to follow the movement of $G_{M1}$ into the cell. Any protein present in the same compartment as CTB–HRP will be polymerized into insoluble aggregates in the presence of membrane-soluble DAB and $H_2O_2$ but not in the absence of $H_2O_2$. The insoluble polymers can be removed by centrifugation, and thus the absence of a protein in the lysate indicates its presence in CTB–HRP-containing compartments. As detailed elsewhere, the HRP-mediated polymerization of proteins depends on the presence of the protein, HRP, DAB, and $H_2O_2$ in the same subcellular compartment, and nonspecific, promiscuous polymerization of proteins outside HRP-containing compartments is not observed (9, 45). The movement of $G_{M1}$ from the plasma membrane into early endosomes and to the IIPLC was followed. To detect the movement of CTB–HRP into early endosomes, the TfR was monitored. TfR has been shown by others to be excluded from lipid rafts (35). B cells were surface biotinylated and incubated at 4°C with CTB–HRP in the presence or absence of anti-Ig. The cells were washed and warmed to 37°C for varying lengths of time up to 120 min. At the end of each time point, the cells were exposed to the chemical cross-linking reagent DAB in the presence or absence of $H_2O_2$ and lysed, and the lysates were centrifuged to remove insoluble polymers. TfR was immunoprecipitated from the cleared lysate and subjected to SDS-PAGE and immunoblot probing for biotinylated proteins using streptavidin–HRP. In cells in which the BCR was not cross-linked, CTB–HRP briefly contacts ~50% of TfRs after warming to 37°C and by 30 min is in contact with a steady state level of ~20% of the biotinylated TfRs (Fig. 5). Because it is difficult to rule out the presence of aggregated or multimerized CTB in the CTB–HRP conjugate preparation, it is not possible to be certain that the observed contact of the CTB–HRP with TfR reflects the constitutive behavior of $G_{M1}$ or whether the contact with TfR is induced by aggregated CTB–HRP. In B cells in which the BCR is cross-linked, CTB–HRP appears to contact more of the TfR upon warming to 37°C (>90%) and to stay in contact with the TfR longer (>60 min) before returning to steady state levels of 20% by 120 min. The kinetics of contact of CTB–HRP with the TfR after BCR cross-linking are similar to those previously observed for BCR contact with the TfR after BCR cross-linking (45).

To determine if any $G_{M1}$ is targeted to the IIPLC, B cells were pulsed for 15 min with [$^{35}$S]methionine in the presence of CTB–HRP and in the presence or absence of anti-Ig. The cells were washed, warmed to 37°C, and chased for 60–180 min. Times were selected that allowed for the detection of newly assembled class II molecules that first bind peptide and adopt SDS-stable conformation in the IIPLC, ~60–90 min after synthesis (9, 46). At the end of each chase time, the cells were treated with DAB in the presence or absence of $H_2O_2$ to cross-link proteins present in the same compartment as the CTB–HRP. The lysates were centrifuged to remove insoluble cross-linked polymers, and class II molecules were immunoprecipitated from the cleared lysate. In untreated B cells, SDS-stable class II heterodimers first appear faintly at 60 min of chase and continue to increase over 150 min and then decrease by 180 min as the

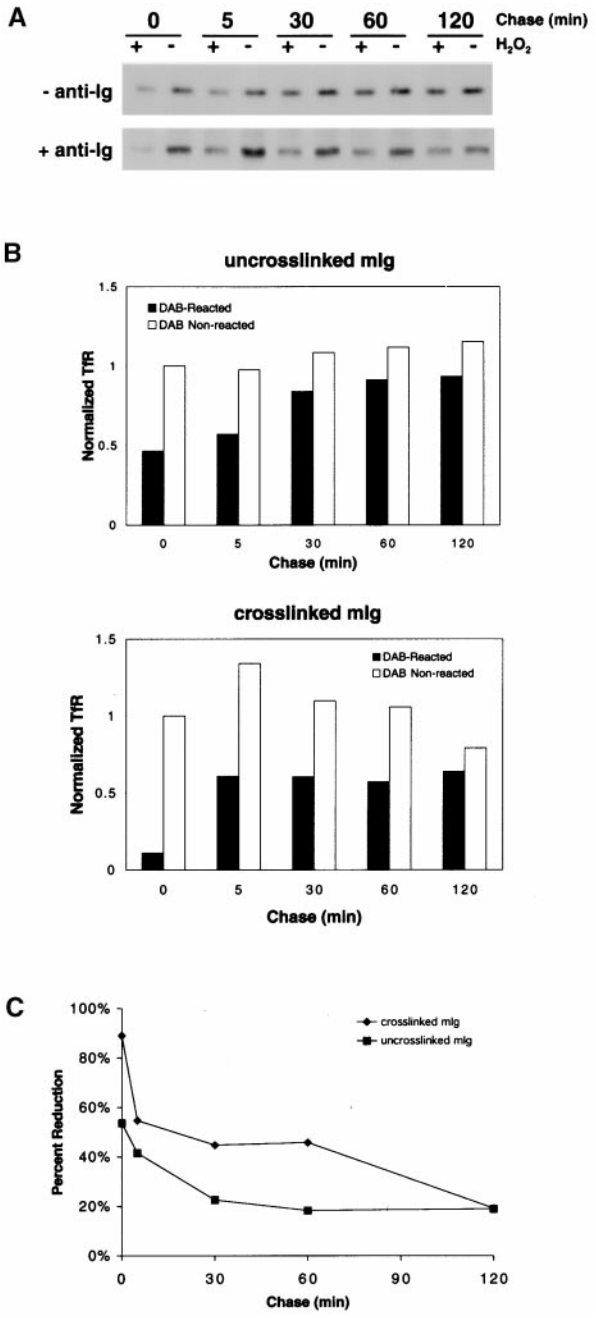


**Figure 5.** BCR cross-linking results in CTB–HRP internalization into TfR-positive early endosomes. (A) CH27 cells were surface biotinylated, incubated at 4°C with CTB–HRP in the presence or absence of anti-Ig, and chased for various times. At the end of each time point, the cells were incubated with DAB in the presence or absence of $H_2O_2$ and lysed in RIPA lysis buffer, and insoluble polymers were removed by centrifugation. TfR was immunoprecipitated from the lysate supernatants and subjected to 10% SDS-PAGE and immunoblot probing for biotinylated proteins using streptavidin–HRP and ECL. (B) The TfR bands from at least three separate experiments were quantified by densitometry, and the average amounts of TfR were normalized to the amount present in cells at 0 min treated with DAB without $H_2O_2$. (C) The amounts of TfR presented in B are shown as percent reduction in DAB-reacted cells at each time point.

class II molecules exit the IIPLC and traffic to the plasma membrane (Fig. 6). The intense band above the class II $\alpha/\beta$ dimers present at 60 min and decreasing thereafter has been previously determined to contain Ii dimers. Significantly, the amount of SDS-stable class II molecules formed was equivalent at each time point in the presence or absence of $H_2O_2$ (Fig. 6), indicating that CTB–HRP was not present in the peptide loading compartment. In contrast, in B cells in which the BCR was cross-linked, the number of SDS-stable class II molecules was decreased in the presence of $H_2O_2$ beginning after 90 min of chase time. The reduction of SDS-stable class II molecules was maximal (~30%) at 120–150 min and less by 180 min as class II molecules exited the peptide loading compartment.

Taken together, these results indicate that in unactivated B cells, the CTB–HRP bound to $G_{M1}$ briefly enters early endocytic TfR-containing compartments but is not targeted to the late IIPLC. Cross-linking the BCR, which, as shown previously, results in BCR targeting to the IIPLC (9, 45), results in a concomitant targeting of $G_{M1}$-bound CTB–HRP to the IIPLC. $G_{M1}$ appears to stay in contact with the BCR en route to the IIPLC, as shown by the ability of CTB–HRP to cause Ig$\alpha$ polymerization throughout the chase period (data not shown). Thus, the BCR appears to remain associated with a portion of the lipid raft $G_{M1}$ as the BCR is targeted to the IIPLC.

*The GPI-linked Ig Mutant μCytoΔ Is Constitutively Concentrated in Lipid Rafts but Is Not Targeted to the IIPLC.* The results presented above showed that the BCR is excluded from lipid rafts in unactivated cells and upon cross-linking is translocated into lipid rafts and targeted to the IIPLC. The targeting of the BCR to the IIPLC was accompanied by the movement of a portion of the lipid raft $G_{M1}$ to the IIPLC. To determine the relationship between residency of a receptor in lipid rafts and targeting to the IIPLC, we analyzed a human Ig, μCytoΔ, in which the cytoplasmic domain was deleted. Previous characterization showed that μCytoΔ stably transfected into mouse A20 cells (A20μCytoΔ) is expressed as a GPI-linked protein that does not associate with the Ig$\alpha$/Ig$\beta$ complex (13, 14). As a GPI-linked protein, μCytoΔ is predicted to reside in lipid rafts. The behavior of μCytoΔ was compared with that of the endogenous mouse Ig in A20μCytoΔ cells and to that of a WT human Ig (μWT) in A20μWT cells. By flow cytometry, both μCytoΔ (cytoplasmic tail deletion) and μWT are expressed at levels similar to that of the endogenous mouse Ig in both cell lines (Fig. 7 A). The staining is specific, and the cells do not stain using FITC-labeled antibodies specific for the human $\gamma$ chain. The cell surface expression of μCytoΔ as a GPI-linked protein was verified by PI-PLC treatment of biotinylated cells followed by immunoprecipitation of human IgM and immunoblot analysis, probing for biotinylated proteins. Upon treatment with PI-PLC, μCytoΔ is released into the supernatant, in contrast to μWT, which remains cell associated (Fig. 7 B).

The lipid raft localization of μCytoΔ, μWT, and endogenous mouse IgG was determined using HRP-conjugated antibodies as described above. In brief, A20μCytoΔ

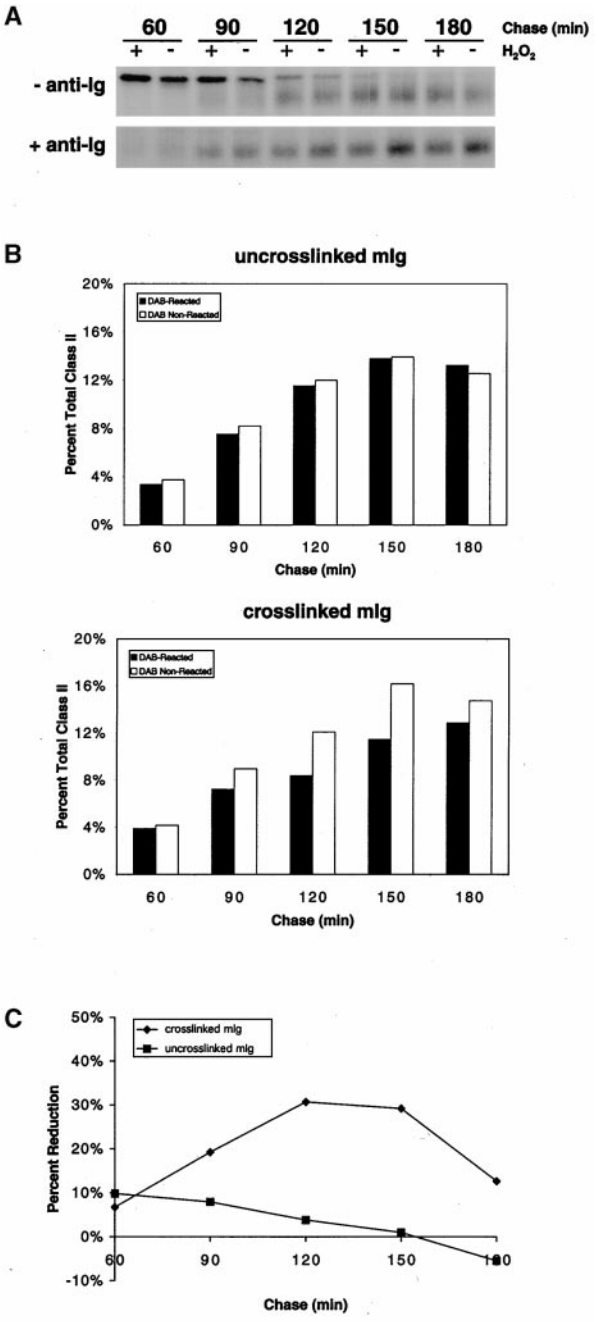


**Figure 6.** BCR cross-linking results in CTB–HRP targeting to the class II peptide loading compartment. (A) CH27 cells were labeled with [$^{35}$S]methionine for 15 min in the presence of CTB–HRP and in the presence or absence of anti-Ig and chased for 60–180 min. At the end of each time point, the cells were treated with DAB in the presence or absence of $H_2O_2$ and lysed in 1% Triton X-100 lysis buffer, and insoluble polymers were removed by centrifugation. The I-$E^k$ class II molecules were immunoprecipitated from the lysate and subjected to SDS-PAGE without boiling or reducing the samples, conditions under which peptide-bound class II $\alpha/\beta$ dimers are stable. (B) The $\alpha/\beta$ dimer bands of at least three independent experiments were quantified by densitometry, and the average amounts for each chase time are shown as the percent of the total amount of SDS-stable class II immunoprecipitated from all time points. (C) The amount of SDS-stable class II presented in B is shown as the percent reduction in DAB-reacted cells at each time point.

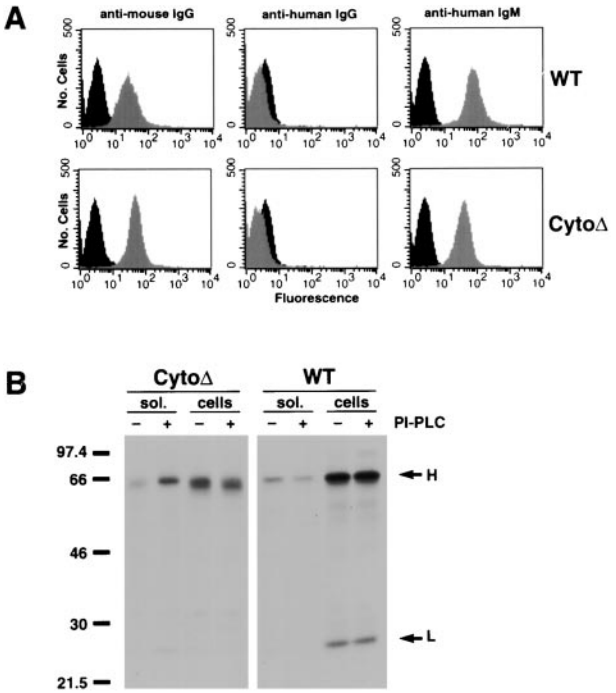


**Figure 7.** Cytoplasmic tail deletion Ig mutation is expressed on the cell surface as a GPI-linked protein. (A) A20μCytoΔ and A20μWT cells were analyzed by flow cytometry using FITC-labeled antibodies specific for mouse IgG, human IgG, and human IgM (gray shaded areas). Also shown as controls are the stainings of human 114 cells with FITC-labeled anti–mouse IgG and nontransfected A20 cells with FITC-labeled anti–human IgG and anti–human IgM (black shaded areas). (B) Cells were surface biotinylated and untreated or treated with PI-PLC at 37°C for 1 h. Solubilized proteins in the supernatant and lysates from the cell pellets were immunoprecipitated for human Ig, and the immunoprecipitates were subjected to 10% SDS-PAGE and immunoblot probing for biotinylated proteins using streptavidin–HRP and ECL.

or A20μWT cells were untreated or incubated with HRP-conjugated antibodies specific for either mouse IgG or human IgM for 1 h at 4°C. The cells were washed and warmed to 37°C for 30 min, lysed in 1% Triton X-100 lysis buffer, and subjected to discontinuous sucrose density gradient centrifugation. The HRP activity in the individual gradient fractions was measured. The endogenous peroxidase activity in the untreated cells is low in the lipid raft region of the gradient and only slightly higher in the soluble membrane fractions at the bottom of the gradient (Fig. 8 A). The HRP-coupled antibodies specific for the endogenous mouse IgG were present in both the lipid raft region of the gradient and the soluble membrane region at the bottom of the gradient. The behavior of μWT was similar to that of mouse IgG after HRP–anti-Ig treatment, distributing both in the raft region and in the detergent-soluble region of the sucrose gradient (Fig. 8 A). These patterns were similar to that observed for mouse IgM in CH27 cells. In contrast, HRP-conjugated antibodies specific for human IgM in A20μCytoΔ cells were located exclusively in the lipid raft region of the gradient.

To independently confirm the location of μCytoΔ with regard to lipid rafts, A20μCytoΔ cells were either un-

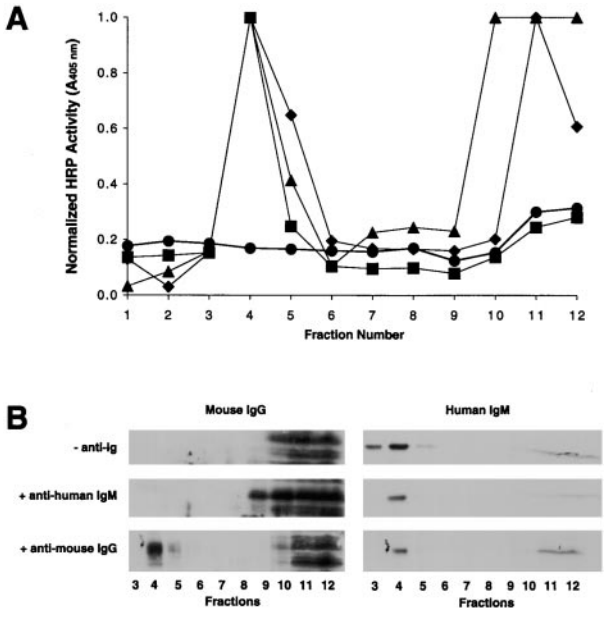


**Figure 8.** Cytoplasmic tail deletion mutants of sIg are localized in lipid rafts in resting cells. (A) A20μCytoΔ and A20μWT cells were incubated with HRP-conjugated rabbit anti–human IgM or goat anti–mouse IgG for 1 h at 4°C, washed, and chased for 30 min. The cells were then lysed in 1% Triton X-100 in TNEV buffer, and the lysates were subjected to discontinuous sucrose density gradient centrifugation. Fractions were collected and HRP activity measured. Shown are untreated A20μCytoΔ (●), A20μCytoΔ treated with HRP–anti–human Ig (■) or HRP–anti–mouse Ig (◆), and A20μWT treated with HRP–anti–human Ig (▲). Shown is a representative experiment of three independent experiments. (B) A20μCytoΔ cells were treated with either anti–human IgM or anti–mouse IgG at 4°C for 1 h, washed, and warmed to 37°C for 30 min. The cells were lysed in 1% Triton X-100 in TNEV buffer and subjected to discontinuous sucrose gradient centrifugation. The gradient fractions were analyzed by 10% SDS-PAGE and immunoblot probing with either mouse IgG– or human IgM–specific antibodies and ECL.

treated or incubated with antibodies specific for mouse IgG or human IgM at 4°C for 1 h, washed, and incubated at 37°C for 30 min. The cells were lysed in 1% Triton X-100 in TNEV buffer and fractionated on a discontinuous sucrose gradient, and the fractions were subjected to SDS-PAGE and immunoblot probing for either mouse IgG or human IgM. The mouse IgG is not present in the lipid raft region of the gradient in unactivated A20μCytoΔ cells (Fig. 8 B), and upon cross-linking, mouse IgG translocates to the lipid rafts. This result is similar to that described above for mouse IgM in CH27 cells and indicates that the heavy chain isotype of the sIg does not influence its behavior with regard to lipid raft localization. In cells treated with antibodies specific for human IgM, mouse IgG remains excluded from the lipid raft region. Thus, cross-linking μCytoΔ had no effect on endogenous mouse IgG. In contrast to the behavior of endogenous mouse IgG, human μCytoΔ is found nearly exclusively in the lipid raft region in unactivated cells (Fig. 8 B). Upon cross-linking using antibodies specific for human IgM, the position of μCytoΔ in lipid rafts does not change. Moreover, the cross-linking and translocation of the mouse IgG into lipid rafts does not alter the position of μCytoΔ.

To determine if the inclusion of μCytoΔ in the buoyant fractions was dependent upon the integrity of the lipid rafts and to determine if aggregation of the receptor alone dictates its behavior on sucrose gradients, A20μCytoΔ cells were treated with anti-Ig and the cholesterol-sequestering drug methyl-β-cyclodextrin that disrupts cholesterol-dependent rafts. In cyclodextrin-treated cells, μCytoΔ is no longer present in the buoyant region of the sucrose gradient but rather in the Triton X-100–soluble dense region of the gradient, even in the presence of cross-linking antibody (Fig. 9). The effect of cyclodextrin was partially reversible after 3 h with the addition of cholesterol (Fig. 9). Taken together, these results indicate that the localization in buoyant regions of the sucrose gradient is dependent on the integrity of the lipid rafts, and aggregation of sIg with anti-Ig alone does not result in appearance of the sIg in the buoyant gradient functions.

To determine if the μCytoΔ is targeted to the IIPLC after cross-linking, A20μCytoΔ cells were pulsed with [$^{35}$S]methionine for 15 min in the presence of HRP-conjugated antibodies specific for either mouse IgG or human IgM. The cells were washed and incubated for 60–180 min at 37°C. At the end of each time point, the cells were treated with DAB in the presence or absence of $H_2O_2$ and lysed, and the I-$A^d$ class II molecules were immunoprecipitated. The immunoprecipitates were subjected to SDS-PAGE without reducing or boiling the samples, conditions under which peptide-bound class II α/β dimers are stable. In cells treated with HRP–anti–mouse IgG, the number of class II α/β dimers is decreased after treatment with DAB plus $H_2O_2$ as compared with DAB alone (Fig. 10). The reduction in class II molecules is observed at 60 min, reaches a maximum of 40% at 120 min, and decreases thereafter as the class II molecules exit the IIPLC. Similar results were obtained by ana-

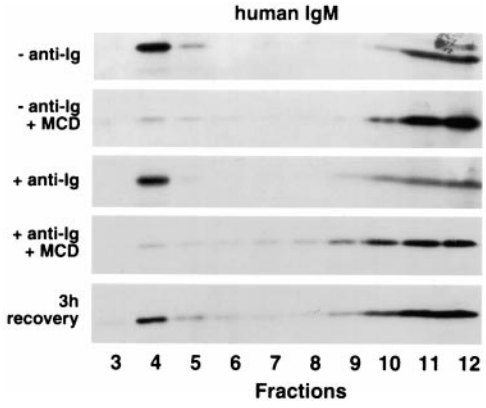


**Figure 9.** Disruption of lipid rafts results in the reversible loss of μCytoΔ from the detergent-insoluble region of the sucrose gradient. A20μCytoΔ cells were untreated or pretreated with 12.5 mM methyl-β-cyclodextrin for 20 min at 37°C and washed to remove drug–cholesterol complexes. Half of the cells were removed and placed in 15% CM for 3 h to allow for cholesterol recovery. Cells were then treated with anti–human IgM, lysed in 1% Triton X-100 in TNEV, and subjected to discontinuous sucrose gradient centrifugation. Fractions were analyzed by 10% SDS-PAGE and immunoblot probing with HRP-labeled human IgM–specific antibodies and ECL. Shown are representative blots from three independent experiments.

lyzing μWT in A20μWT cells using HRP–anti–human IgM, in which case 25% of newly synthesized SDS-stable class II molecules were cross-linked after 120 min of chase time. These results are in agreement with those previously shown for the contact of WT IgM BCR with newly synthesized I-$E^k$ in CH27 cells (9, 45). In contrast, in A20μCytoΔ cells treated with HRP–anti–human IgM, there was no reduction in the number of class II molecules in cells treated with DAB plus $H_2O_2$ as compared with DAB alone (Fig. 10). Moreover, in A20μCytoΔ cells treated with antibodies specific for mouse IgG and HRP-conjugated antibodies specific for human IgM, μCytoΔ was not targeted to the IIPLC (data not shown). Thus, μCytoΔ resident in the lipid raft did not accompany the WT mouse BCR to the IIPLC. These findings indicate that the human IgM that constitutively resides in the lipid rafts is not targeted to the IIPLC after cross-linking, in agreement with previous results showing that the μCytoΔ did not target antigen for class II processing (15). Moreover, these results indicate that residency in the lipid rafts region alone is not sufficient for targeting to the IIPLC.

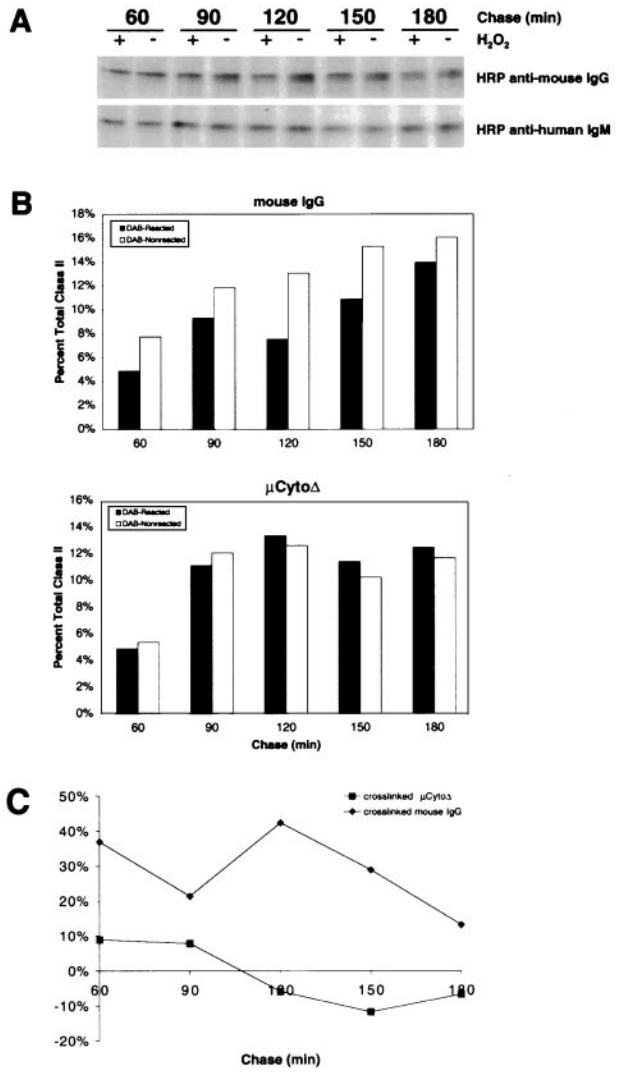


**Figure 10.** Upon cross-linking, μCytoΔ is not targeted to the IIPLC. (A) A20μCytoΔ cells were labeled with [$^{35}$S]methionine for 15 min in the presence of either HRP-conjugated anti–human IgM or anti–mouse IgG, washed, and chased for 60–180 min. At the end of each chase time, the cells were treated with DAB in the presence or absence of $H_2O_2$ and lysed in 1% Triton X-100 lysis buffer. I-$A^d$ class II molecules were immunoprecipitated, analyzed by 10% SDS-PAGE without reducing or boiling the samples, and visualized by autoradiography. (B) The class II α/β dimer bands from three separate experiments were quantified by densitometry, and the average amounts for each chase time are shown as the percent total SDS-stable class II dimers immunoprecipitated from all time points. (C) The amounts of SDS-stable class II presented in B are shown as the percent reduction in DAB-reacted cells at each time point.

## Discussion

The BCR plays two key roles in the B cell response to antigen. The first is to transmit signals through several intracellular pathways that ultimately dictate the fate of the B cell's encounter with antigen (1–3). BCR signaling itself has been recently appreciated to be a complex phenomenon that is directly influenced both positively and negatively by B cell coreceptors, including CD19/CD21, CD22, CD40, and FcγRIIB (1). How the components of the BCR signaling cascade and the coreceptors are organized on the plasma membrane to affect the final outcome is not known. In addition to signaling, the BCR physically transports antigen from the cell surface to the IIPLC (6). The current evidence indicates that the signaling function of the BCR is required to specify both the targeting of the BCR to the IIPLC and the rate at which the targeting is achieved.

How the signaling and targeting functions of the BCR are coordinated is not known. In this report, we show that after cross-linking, the BCR is rapidly translocated into lipid rafts that contain the Src family kinase Lyn, a key kinase in the initiation of the BCR signal transduction cascade, and exclude the phosphatase CD45R. Moreover, we show that phosphorylated Igα and Lyn are present in the lipid rafts after BCR cross-linking. Taken together, these results suggest that the recruitment of the BCR to the lipid rafts may represent an important, previously unappreciated event in BCR signaling, allowing the concentration of the BCR and the enzymes and adaptors of the signaling pathway.

Upon BCR cross-linking, it has been observed that sIg becomes associated with the actin cytoskeleton and that cytoskeletal attachment is not dependent on Igα/β signaling (47). Furthermore, sIg with cytoplasmic tail sequence KVK replaced with the Igα tail was shown to have reduced ability to associate with cytoskeletal actin (48). Although the significance of cytoskeletal attachment remains unknown, we provide evidence that the WT BCR translocated into the lipid raft, along with the raft component $G_{M1}$, is subsequently targeted to the IIPLC in an accelerated fashion. Thus, the lipid raft may provide components necessary for the correct and accelerated targeting of the BCR to the IIPLC. Our result showing that μCytoΔ is constitutively localized in lipid rafts but is not targeted to the IIPLC suggests that raft localization alone is not sufficient for efficient internalization and proper intracellular targeting. Targeting may require initiation of signaling, a function for which μCytoΔ is deficient. However, rafts may provide a means for efficient

cytoskeletal association of sIg either directly or through associated factors. Taken together, the results presented here are consistent with the hypothesis that lipid rafts serve as platforms for both signaling and trafficking of membrane receptors (16).

The molecular mechanisms by which the BCR is translocated to lipid rafts remain to be elucidated. The translocation of the BCR to lipid rafts was nearly instantaneous after cross-linking. The rapidity of the translocation was similar to that reported by Montixi et al. (36), who showed that the engagement of the TCR triggers an immediate accumulation of the TCR and protein tyrosine kinases to lipid rafts, readily detectable within 10 s. Cross-linking the BCR may result in a conformational change of some sort in the BCR that allows its rapid translocation into lipid rafts by destabilizing its interaction with Igα/Igβ or the replacement of Igα/Igβ by some other membrane component. Indeed, Vilen et al. (49) recently provided evidence that after antigen binding, the sIg–Igα/Igβ complex is destabilized such that Igα/Igβ no longer coimmunoprecipitates with sIg. However, the results presented here show that both sIg and Igα enter the rafts, indicating that the BCR remains intact after cross-linking. A conformational change could also be the result of a specific phosphorylation event on one of the tyrosines within the Igα/Igβ ITAMs. Presumably, such a phosphorylation event is insufficient to initiate significant downstream signaling before translocation to the lipid rafts. The current evidence concerning the mechanism of the translocation of the TCR into lipid rafts upon TCR engagement suggests that phosphorylation of the TCR outside the lipid rafts promotes translocation. Alternatively, a conformational change could be induced by the clustering or aggregation of the BCR by cross-linking. Analysis of additional BCR constructs in which both the association of sIg with Igα and Igβ and the signaling potential of the Igα/Igβ complex are altered should be informative with regard to the molecular basis of the trigger that leads to BCR translocation.

The BCR is similar to two other immune receptors in its behavior on the plasma membrane after cross-linking, namely the TCR and the IgE receptor, both of which become concentrated in lipid rafts after engagement. Given that these receptors share many common features in terms of the processes by which signal transduction cascades are initiated and regulated, the observation that similar strategies are used to allow concentration of the components of the signaling cascade is perhaps not surprising. As the composition of the lipid rafts is further characterized and the molecular mechanism underlying the triggering of these receptors to translocate to lipid rafts is defined, there are likely to be more commonalities discovered as well as interesting differences revealed.

This work was supported by grants from the National Institute of Allergy and Infectious Diseases (AI 27957, AI 18939, and AI 40309) to S.K. Pierce and the National Institute of General Medical Sciences (NIGMS; GM47726) to R.N. Mitchell. P.C. Cheng is supported by a grant from the NIGMS Medical Scientist Training Program (GM08152).

Address correspondence to Susan K. Pierce, 2153 N. Campus Dr., Hogan 3-120, Evanston, IL 60208. Phone: 847-491-5089; Fax: 847-467-1610; E-mail: skpierce@nwu.edu

*Submitted: 8 March 1999 Revised: 27 September 1999 Accepted: 27 September 1999*

## References

1. Reth, M., and J. Wienands. 1997. Initiation and processing of signals from the B cell antigen receptor. *Annu. Rev. Immunol.* 15:453–479.
2. Pleiman, C.M., D. D'Ambrosia, and J.C. Cambier. 1994. The B-cell antigen receptor complex: structure and signal transduction. *Immunol. Today*. 15:393–399.
3. Gold, M.R., and A.L. DeFranco. 1994. Biochemistry of B lymphocyte activation. *Adv. Immunol.* 55:221–295.
4. Parker, D.C. 1993. T cell-dependent B cell activation. *Annu. Rev. Immunol.* 11:331–360.
5. Germain, R.N. 1994. MHC-dependent antigen processing and peptide presentation: providing ligands for T lymphocyte activation. *Cell.* 76:287–299.
6. Watts, C. 1997. Capture and processing of exogenous antigens for presentation on MHC molecules. *Annu. Rev. Immunol.* 15:821–850.
7. Wagle, N.M., P. Cheng, J. Kim, T.W. Sproul, K.D. Kausch, and S.K. Pierce. 1999. B lymphocyte signaling receptors and the control of class II antigen processing. *Curr. Top. Microbiol. Immunol.* 245:101–126.
8. Casten, L.A., and S.K. Pierce. 1988. Receptor-mediated B cell antigen processing: increased antigenicity of a globular protein covalently coupled to antibodies specific for B cell surface structures. *J. Immunol.* 140:404–410.
9. Song, W., H. Cho, P. Cheng, and S.K. Pierce. 1995. Entry of the B-cell antigen receptor and antigen into the class II peptide-loading compartment is independent of receptor cross-linking. *J. Immunol.* 155:4255–4263.
10. Wagle, N.M., J.H. Kim, and S.K. Pierce. 1998. Signaling through the B cell antigen receptor regulates discrete steps in the antigen processing pathway. *Cell. Immunol.* 184:1–11.
11. Aluvihare, V.R., A.A. Khamlichi, G.T. Williams, L. Adorini, and M.S. Neuberger. 1997. Acceleration of intracellular targeting of antigen by the B-cell antigen receptor: importance depends on the nature of the antigen-antibody interaction. *EMBO (Eur. Mol. Biol. Organ.) J.* 16:3553–3562.
12. Shaw, A.C., R.N. Mitchell, Y.K. Weaver, J. Campos-Torres, A.K. Abbas, and P. Leder. 1990. Mutations of immunoglobulin transmembrane and cytoplasmic domains: effect on intracellular signalling and antigen presentation. *Cell.* 63:381–392.
13. Mitchell, R.N., A.C. Shaw, Y.K. Weaver, P. Leder, and A.K. Abbas. 1991. Cytoplasmic tail deletion converts mem-

brane immunoglobulin to a phosphatidylinositol-linked form lacking signaling and efficient antigen internalization functions. *J. Biol. Chem.* 266:8856–8860.
14. Grupp, S.A., K. Campbell, R.N. Mitchell, J.C. Cambier, and A.K. Abbas. 1993. Signaling-defective mutants of the B lymphocyte antigen receptor fail to associate with Ig-α and Ig-β/γ. *J. Biol. Chem.* 268:776–779.
15. Mitchell, R.N., K.A. Barnes, S.A. Grupp, M. Sanchez, Z. Misulovin, C. Nussenzweig, and A.K. Abbas. 1995. Intracellular targeting of antigens internalized by membrane immunoglobulin in B lymphocytes. *J. Exp. Med.* 181:1705–1714.
16. Simons, K., and E. Ikonen. 1997. Functional rafts in cell membranes. *Nature.* 387:569–572.
17. Brown, D.A., and J.K. Rose. 1992. Sorting of GPI-anchored proteins to glycolipid-enriched membrane subdomains during transport to the apical cell surface. *Cell.* 68:533–544.
18. Kurzchalia, T.V., E. Hartman, and P. Dupree. 1995. Guilt by insolubility—does a protein's detergent insolubility reflect a caveolar location? *Trends Cell Biol.* 5:187–189.
19. Parton, R.G., and K. Simons. 1995. Digging into caveolae. *Science.* 269:1398–1399.
20. Rodgers, W., and J.K. Rose. 1996. Exclusion of CD45 inhibits activity of $p56^{lck}$ associated with glycolipid-enriched membrane domains. *J. Cell Biol.* 135:1515–1523.
21. Fra, A.M., M. Masserini, P. Palestini, S. Sonnino, and K. Simons. 1995. A photo-reactive derivative of ganglioside GM1 specifically cross-links VIP21-caveolin on the cell surface. *FEBS Lett.* 375:11–14.
22. Mayor, S., and F.R. Maxfield. 1995. Insolubility and redistribution of GPI-anchored proteins at the cell surface after detergent treatment. *Mol. Biol. Cell.* 6:929–944.
23. Scheiffele, P., M.G. Roth, and K. Simons. 1997. Interaction of influenza virus haemagglutinin with sphingolipid-cholesterol membrane domains via its transmembrane domain. *EMBO (Eur. Mol. Biol. Organ.) J.* 16:5501–5508.
24. Field, K.A., D. Holowka, and B. Baird. 1997. Compartmentalized activation of the high affinity immunoglobulin E receptor within membrane domains. *J. Biol. Chem.* 272:4276–4280.
25. Stauffer, T.P., and T. Meyer. 1997. Compartmentalized IgE receptor-mediated signal transduction in living cells. *J. Cell Biol.* 139:1447–1454.
26. Deans, J.P., S.M. Robbins, M.J. Polyak, and J.A. Savage. 1998. Rapid redistribution of CD20 to a low density detergent-insoluble membrane compartment. *J. Biol. Chem.* 273:344–348.
27. Li, S., T. Okamoto, M. Chun, M. Sargiacomo, J.E. Casanova, S.H. Hansen, I. Nishimoto, and M.P. Lisanti. 1995. Evidence for a regulated interaction between heterotrimeric G proteins and caveolin. *J. Biol. Chem.* 270:15693–15701.
28. Casey, P.J. 1995. Protein lipidation in cell signaling. *Science.* 268:221–224.
29. Lisanti, M.P., P.E. Scherer, J. Vidugiriene, Z. Tang, A. Hermanowski-Vosatka, Y.H. Tu, R.F. Cook, and M. Sargiacomo. 1994. Characterization of caveolin-rich membrane domains isolated from an endothelial-rich source: implications of human disease. *J. Cell Biol.* 126:111–126.
30. Harder, T., R. Kellner, R.G. Parton, and J. Gruenberg. 1997. Specific release of membrane-bound annexin II and cortical cytoskeletal elements by sequestration of membrane cholesterol. *Mol. Biol. Cell.* 8:533–545.
31. Fujimoto, T. 1996. GPI-anchored proteins, glycosphingolipids, and sphingomyelin are sequestered to caveolae only after crosslinking. *J. Histochem. Cytochem.* 44:929–941.
32. Varma, R., and S. Mayor. 1998. GPI-anchored proteins are organized in submicron domains at the cell surface. *Nature.* 394:798–801.
33. Friedrichson, T., and T.V. Kurzchalla. 1998. Microdomains of GPI-anchored proteins in living cells revealed by crosslinking. *Nature.* 394:802–805.
34. Harder, T., and K. Simons. 1997. Caveolae, DIGs, and the dynamics of sphingolipid-cholesterol microdomains. *Curr. Opin. Cell Biol.* 9:534–542.
35. Harder, T., P. Scheiffele, P. Verkade, and K. Simons. 1998. Lipid domain structure of the plasma membrane revealed by patching of membrane components. *J. Cell Biol.* 141:929–942.
36. Montixi, C., C. Langlet, A.-M. Bernard, J. Thimonier, C. Dubois, M.-A. Wurbel, J.-P. Chauvin, M. Pierres, and H.-T. He. 1998. Engagement of T cell receptor triggers its recruitment of low-density detergent-insoluble membrane domains. *EMBO (Eur. Mol. Biol. Organ.) J.* 17:5334–5348.
37. Xavier, R., T. Brennan, Q. Li, C. McCormack, and B. Seed. 1998. Membrane compartmentation is required for efficient T cell activation. *Immunity.* 8:723–732.
38. Moran, M., and M.C. Miceli. 1998. Engagement of GPI-linked CD48 contributes to TCR signals and cytoskeletal reorganization: a role for lipid rafts in T cell activation. *Immunity.* 9:787–796.
39. Zhang, W., R.P. Trible, and L.E. Samelson. 1998. LAT palmitoylation: its essential role in membrane microdomain targeting and tyrosine phosphorylation during T cell activation. *Immunity.* 9:239–246.
40. Viola, A., S. Schroeder, Y. Sakakibara, and A. Lanzavecchia. 1999. T lymphocyte costimulation mediated by reorganization of membrane microdomains. *Science.* 283:680–682.
41. Jelachich, M.L., M.J. Grusby, D. Clark, D. Tasch, E. Margoliash, and S.K. Pierce. 1984. Synergistic effects of antigen and soluble T-cell factors in B-lymphocyte activation. *Proc. Natl. Acad. Sci. USA.* 81:5537–5541.
42. Kilmartin, J.V., B. Wright, and C. Milstein. 1982. Rat monoclonal antitubulin antibodies derived by using a new nonsecreting rat cell line. *J. Cell Biol.* 93:576–582.
43. Goldstein, J.L., S.K. Basu, and M.S. Brown. 1983. Receptor-mediated endocytosis of low-density lipoprotein in cultured cells. *Methods Enzymol.* 98:241–260.
44. Schafer, P.H., J.M. Green, S. Malapati, L. Gu, and S.K. Pierce. 1996. HLA-DM is present in one-fifth the amount of HLA-DR in the class II peptide-loading compartment where it associates with leupeptin-induced peptide (LIP)-HLA-DR. *J. Immunol.* 157:5487–5495.
45. Cheng, P.C., C.R. Steele, L. Gu, W. Song, and S.K. Pierce. 1999. MHC class II antigen processing in B cells: accelerated intracellular targeting of antigens. *J. Immunol.* 162:7171–7180.
46. Schafer, P.H., and S.K. Pierce. 1994. Evidence for dimers of MHC class II molecules in B lymphocytes and their role in low affinity T cell responses. *Immunity.* 1:699–707.
47. Hartwig, J.H., L.S. Jugloff, N.J. DeGroot, S.A. Grupp, and J. Jongstra-Bilen. 1995. The ligand-induced membrane IgM association with the cytoskeletal matrix of B cells is not mediated through the Ig αβ heterodimer. *J. Immunol.* 155:3769–3779.
48. Park, J.Y., and J. Jongstra-Bilen. 1997. Interactions between membrane IgM and the cytoskeleton involve the cytoplasmic domain of the immunoglobulin receptor. *Eur. J. Immunol.* 27:3001–3009.
49. Vilen, B.J., T. Nakamura, and J.C. Cambier. 1999. Antigen-stimulated dissociation of BCR mIg from Ig-α/Ig-β: implications for receptor desensitization. *Immunity.* 10:239–248.